IEEE Access
Multidisciplinary | Rapid Review | Open Access Journal

Received 11 March 2023, accepted 10 May 2023, date of publication 16 May 2023, date of current version 24 May 2023.

Digital Object Identifier 10.1109/ACCESS.2023.3276751

RESEARCH ARTICLE

A Novel Optimal Voltage Vector Selection Control Strategy for Vienna Rectifier

YONGMING SUN, XINGTIAN FENG, ZHANJIANG DAI, AND WENZHONG MA
College of New Energy, China University of Petroleum (East China), Qingdao 266580, China

Corresponding author: Xingtian Feng (topfxt@163.com)

This work was supported in part by the National Natural Science Foundation of China under Grant 51977220, and in part by the Natural Science Foundation of Shandong Province under Grant ZR2019MEE094.

ABSTRACT At present, model predictive control (MPC) is widely used in power electronic converters. The objective function is typically utilized to select the optimal voltage vector, but the switching frequency is not fixed or too high during the selection process. Therefore, to address this issue, a novel optimal voltage vector selection control strategy for Vienna rectifier is proposed in this paper. Specifically, hysteresis link is introduced into finite control set-model predictive direct power control (FCS-MPDPC). The optimization criterion is changed from the traditional objective function tracking error minimization to the longest extension step in the hysteresis loop. As a result, the switching frequency can be reduced and the control algorithm can be simplified by redefining the optimization criteria of the rectifier output voltage vector. Moreover, according to the power control model of Vienna rectifier, three-level space vector pulse width modulation (SVPWM) is used to generate the switching function for the next cycle. Finally, an experimental platform for Vienna rectifier based on dSPACE hardware is built to verify the feasibility of the proposed strategy. Experimental results show that the control strategy can ensure the rectifier to run normally and exhibit good steady state performance.

INDEX TERMS Vienna rectifier, optimal voltage vector selection, finite control set-model predictive direct power control, extension step, switching frequency.

I. INTRODUCTION

The three-phase three-wire Vienna rectifier is an efficient and stable three-level rectifier device. Compared with the traditional two-level rectifier, Vienna rectifier can achieve higher power factor and higher efficiency during operation. Furthermore, in comparison to the traditional three-level rectifier, the Vienna has a simple structure and no bridge arm pass-through and dead zone problems, making it widely used in automobile charging piles, wind power generation, and uninterruptible power supply systems, among others. Further study and analysis of the Vienna rectifier will be beneficial for its improvement and development, as well as for its high research value [1], [2], [3].

In finite control set-model predictive control (FCS-MPC), the objective function can make the predicted value accurately track the reference value at the next moment, thereby minimizing the tracking error and achieving the goal. When there are multiple control objectives in the system, weight factors are included in the objective function to regulate each objective. When designing the weight factor, specific goals can be focused on according to different system requirements. There is also a certain coupling relationship between each target, and altering the weight factor of one target will affect the system's control effect on the other targets.

Reference [4] has sorted out common objective functions for converters, however, these have been limited to a single control objective. Reference [5] introduces the allocation of weight factors when considering multiple control objectives in the system. Reference [6] optimized the weight factor allocation and minimized the torque ripple by calculating it, thereby suppressing the torque ripple. Reference [7] added the concept of ranking to the model prediction to eliminate

The associate editor coordinating the review of this manuscript and approving it for publication was Tariq Masood.

the weight factor between control objectives, however this control strategy can only be applied to systems with two control objectives, making it not universal.

After determining the objective function in traditional FCS-MPC, the alternative vectors in each period should be substituted into the function in order to select the optimal one, the one that can make the objective function minimum is deemed to be the optimal voltage vector, thus obtaining the best operating state of the system. The optimization process is carried out once per period, with no connection between adjacent periods. However, the optimal voltage vector in the next period may be the same as the one in the previous period, leading to an uncertain switching frequency. Furthermore, all alternative vectors must be optimized once in every sampling period, leading to an increase in the system's calculation amount.

In [8], modulation is introduced into the FCS-MPC, enabling the carrier to generate the switching function of the optimal voltage vector, thus realizing fixed frequency control to some extent. Reference [9] proposes a model predictive control method by adding virtual vectors, which are optimized together with the actual vectors and then modulated and applied to the switch. Although this increases the prediction accuracy and realizes the fixed frequency control of the switch, it also increases the calculation amount of the system, thus affecting the system's decision speed. To reduce the computational burden of the system, [10] screens the alternative vectors in the converter. However, by reducing the alternative vectors to simplify the operational control, the optimal voltage vector may be missed, thereby affecting the control effect. Reference [11] applies the concept of deadbeat control to model predictive control, reducing the prediction times in the system operation process, thereby obtaining the reference value of the voltage vector via the predicted value at the next sampling time, equal to the reference value. The objective function selects the voltage vector closest to the reference voltage as the control quantity and requires only one prediction for the whole process, thus reducing the optimization times and solving the problem of large computation. However, when the system is disturbed, the voltage vector obtained by this control method may not be accurate.

This paper proposes a hysteresis-finite control set-model predictive direct power control (H-FCS-MPDPC) strategy for the Vienna rectifier. The optimization criterion of the output voltage vector of the Vienna rectifier is redefined, and the hysteresis link in the hysteresis control is extended to the FCS-MPDPC. By choosing an appropriate bandwidth, the power amplitude is constrained within a given hysteresis loop, and the output vector is kept constant when it does not exceed the bandwidth, thereby allowing the system to operate at a lower switching frequency state. Finally, the proposed control strategy is verified through simulation and experiment. The results show that the contradiction between the switching frequency and the total harmonic distortion (THD) of the input current can be effectively solved by adjusting the hysteresis width of the Vienna rectifier. On the premise of ensuring the normal operation of the rectifier, the proposed strategy has a lower switching frequency than that of the traditional FCS-MPC.

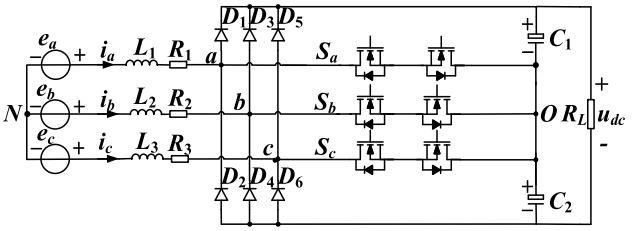

FIGURE 1. Topology of the three-phase Vienna rectifier.

II. VIENNA RECTIFIER MATHEMATICAL MODEL AND VOLTAGE VECTOR

A. TOPOLOGICAL STRUCTURES AND MATHEMATICAL MODELS

The topology of the three-phase three-level Vienna rectifier is shown in Fig. 1. $e_{a,b,c}$ represent the three-phase AC voltage. $i_{a,b,c}$ represent the three-phase input current. $L_{1,2,3}$ are filter inductors of AC side, and their inductance values are all L. $R_{1,2,3}$ are filter resistors, and their resistance values are all R. D_{1-6} are 6 fast recovery diodes. $S_{a,b,c}$ are three-phase switches, each switch is composed of two MOSFET in series in reverse. $C_{1,2}$ are the upper and lower capacitors of the DC side, and their capacitance values are both C. DC side load resistance is R_L. The output voltage is u_{dc}.

According to the topology structure, the mathematical model of three-phase three-level Vienna rectifier can be obtained as follows:

$$e_{a,b,c} = Ri_{a,b,c} + L\frac{di_{a,b,c}}{dt} + (u_{(a,b,c)O} + u_{ON}) \tag{1}$$

B. VOLTAGE VECTOR

Vienna rectifier is a three-level rectifier, the AC side output level has $3^3 = 27$ combination states. Since the output voltage $u_{(a,b,c)O}$ cannot be both $u_{dc}/2$ or $-u_{dc}/2$, there are 25 different switching level combinations left after excluding these two special cases.

The switch function S_i is defined as:

$$S_i = \begin{cases} 0 & S_i \text{ on} \\ 1 & S_i \text{ off } i_i > 0 \\ -1 & S_i \text{ off } i_i < 0 \end{cases} \tag{2}$$

$i = a,b,c$.

The relationship between the output voltage at the AC side and the output voltage at the DC side is:

$$u_{(a,b,c)O} = S_{(a,b,c)}\frac{u_{dc}}{2} \tag{3}$$

The relationship between the neutral point O on the DC side of the capacitor and the neutral point N on the input side is:

$$u_{ON} = -\frac{1}{3}(S_a + S_b + S_c)\frac{u_{dc}}{2} \tag{4}$$

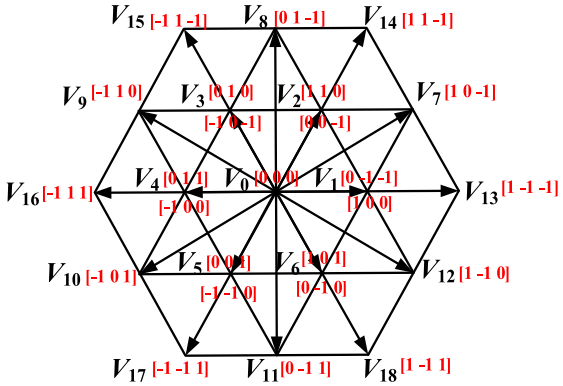

FIGURE 2. Plan of space voltage vector.

According to (3) and (4), the voltage at the clamp site of the rectifier diode relative to the neutral point N of the AC power supply is:

$$u_{(a,b,c)N} = u_{(a,b,c)O} + u_{ON} = (S_{(a,b,c)} - \frac{1}{3}\sum_{i=a,b,c} S_i)\frac{u_{dc}}{2} \tag{5}$$

For different switch combinations, the following voltage space vector plan can be obtained:

It can be seen from Fig. 2 that the space voltage vector plane consists of four basic vectors: the zero vector, the small vector, the medium vector and the large vector. Among them:

(1) The zero vector has only one component, V_0, and its amplitude is 0.

(2) The six small vectors are V_{1-6}, whose amplitude is $u_{dc}/3$.

(3) The six medium vectors are V_{7-12}, whose amplitude is $\sqrt{3}u_{dc}/3$.

(4) The six large vectors are V_{13-18}, whose amplitude is $2u_{dc}/3$.

III. TRADITIONAL OBJECTIVE FUNCTION AND OPTIMAL VOLTAGE VECTOR SELECTION IN FCS-MPDPC

A. FCS-MPDPC IN VIENNA

The application of the FCS-MPDPC to the Vienna rectifier can be divided into the following four steps [12]:

(1) Calculate the instantaneous power and discretize it.

(2) Predict the instantaneous power for the next cycle.

(3) Construct an objective function and obtain optimal voltage vector.

(4) Send the optimal output voltage vector to the SVPWM and generate the corresponding switching signals to act on switching of the rectifier.

The overall control structure is shown in Fig. 3.

The FCS-MPDPC algorithm applied to the Vienna rectifier is simple, has fast dynamic response, and does not require parameter tuning [13], [14], [15]. Firstly, the instantaneous active power and reactive power are obtained:

$$\begin{cases} p = e_\alpha i_\alpha + e_\beta i_\beta \\ q = e_\beta i_\alpha - e_\alpha i_\beta \end{cases} \tag{6}$$

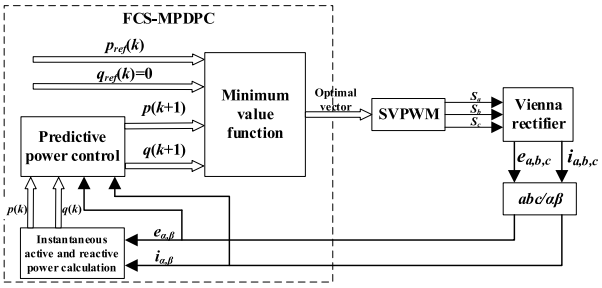

FIGURE 3. Traditional finite control set-model predictive direct power control.

Then, the instantaneous power is discretized, and the predicted value at time $k+1$ is calculated according to the actual value at time k:

$$\begin{cases} p(k+1) = \dfrac{dp}{dt}T + p(k) \\ q(k+1) = \dfrac{dq}{dt}T + q(k) \end{cases} \tag{7}$$

In (7), $(dp/dt)T$ and $(dq/dt)T$ respectively represent the variation of active and reactive power in the k control period.

According to the instantaneous power differential equation in the power control mathematical model of the Vienna rectifier, the active power and reactive power at time $k+1$ can be obtained by substituting (6) into (7) after simplification, as in (8), shown at the bottom of the next page.

B. OBJECTIVE FUNCTION AND OPTIMAL VOLTAGE VECTOR SELECTION

In order to obtain the voltage vector that can make the system run in its optimal state, the predicted value at the next time is typically used as the expected value at the current time, and the standard for constructing the objective function is the minimum sum of squared power errors in each sampling period [16]:

$$J(k) = \lambda_1(p_{ref}(k) - p(k+1))^2 + \lambda_2(q_{ref}(k) - q(k+1))^2 \tag{9}$$

In (9), λ_1 and λ_2 are the weight factors of instantaneous active power and instantaneous reactive power respectively. $p_{ref}(k)$ is the reference value of active power, and $q_{ref}(k)$ is the reference value of reactive power.

Fig. 4 shows the optimization mechanism of the objective function in FCS-MPDPC. At time k, the instantaneous power value is calculated based on the current and voltage values. Then, the predicted instantaneous power values at time $k+1$ under the action of each candidate vector is successively calculated. Finally, the vector with the smallest error from the reference value (it is equal to the magnitude of value J) is selected as the optimal voltage vector of the current time. It can be observed from Fig. 4 that only a single vector can be output in each period and the switching frequency is not fixed [17].

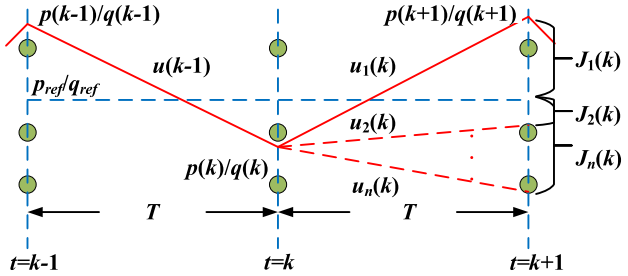

FIGURE 4. Objective function optimization mechanism.

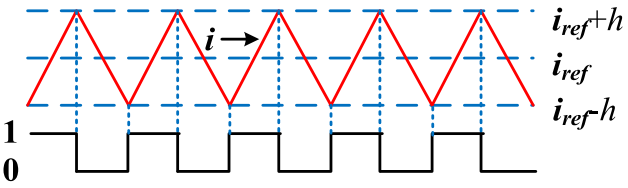

FIGURE 5. Hysteresis current control principle.

IV. NOVEL OPTIMAL VOLTAGE VECTOR SELECTION CONTROL STRATEGY

A. HYSTERESIS WIDTH

The concept of hysteresis width comes from hysteresis control [18], [19], [20]. In traditional hysteresis current control, the input current is compared with the reference current and the switching state of the converter is changed accordingly, based on the error size, in order to keep the phase deviation between the input current and the input voltage within a certain range, thus achieving the purpose of unit power factor operation, which is a typical nonlinear control. At the same time, different hysteresis widths will affect the input current harmonics and the switching frequency. Generally, the larger the hysteresis width, the lower the switching frequency, but the larger the current harmonics. Conversely, the smaller the hysteresis width, the higher the switching frequency, and the smaller the current harmonics. However, being limited by the power switching, the switching frequency cannot be too high [21].

The hysteresis current control principle is shown in Fig. 5. The actual input current is i, the reference current is i_{ref}, and the hysteresis width is set as h. The actual current is compared with the reference current, and the resulting error current is fed into the hysteresis comparator. When the current exceeds the lower hysteresis current limit i_{ref} -h or the upper hysteresis current limit $i_{ref} + h$, the switch will switch according to the given logic to force the current deviation to decrease and thus achieve the effect of current control.

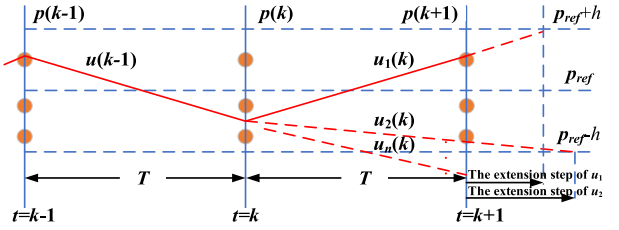

FIGURE 6. Novel optimal voltage vector selection principle.

B. INTRODUCTION OF HYSTERESIS

The novel optimal voltage vector selection control strategy combines the advantages of hysteresis control and FCS-MPDPC. The concept of a hysteresis loop is introduced into the model predictive control [22], and FCS-MPDPC with the hysteresis loop is constructed. With the introduction of the hysteresis loop, the tracking performance and switching frequency of the Vienna rectifier can be easily adjusted by changing the bandwidth, thus enabling the optimization of the control system.

Fig. 6 shows the schematic diagram of the novel voltage vector selection, taking active power as an example. Firstly, the hysteresis width is set as h, and the active power reference value is used as the reference line to construct the hysteresis loop. The upper limit of the hysteresis loop is $p_{ref} + h$, and the lower limit of the hysteresis loop is p_{ref} -h. When the system is located at time k, the active power $p(k)$ at this time can be obtained. Then, the predicted active power value $p(k+1)$ of each candidate vector at time $k+1$ can be obtained from (8). Finally, the predicted power value at time $k+1$ is extended to intersect the upper and lower bounds of the hysteresis ring, and the extension step is obtained. Setting different hysteresis width will affect the distance between the calculated value and the predicted value of the extension line to the boundary, and also affect the step size of the active power. Too small hysteresis width will lead to too small step size, increasing the switching frequency and resulting in switching loss of the system. If the hysteresis width is too large, the power oscillation range of the system will be too large, leading to an increase in the THD of the input current. Therefore, choosing an appropriate hysteresis width will determine the quality of the optimal voltage vector selection. The extended step size can be expressed as:

$$\begin{cases} p_{exten}^{right} = \dfrac{p_{ref} + h - p(k+1)}{p(k+1) - p(k)} \\ p_{exten}^{left} = \dfrac{p_{ref} - h - p(k+1)}{p(k+1) - p(k)} \end{cases} \tag{10}$$

$$\begin{cases} p(k+1) = p(k) \\ \qquad + T[\dfrac{(e_\alpha(k)^2 + e_\beta(k)^2 - e_\alpha(k)u_\alpha(k) - e_\beta(k)u_\beta(k))}{L} - \dfrac{R}{L}p(k) - \omega q(k)] \\ q(k+1) = q(k) \\ \qquad + T[\dfrac{(e_\alpha(k)u_\beta(k) - e_\beta(k)u_\alpha(k))}{L} - \dfrac{R}{L}q(k) + \omega p(k)] \end{cases} \tag{8}$$

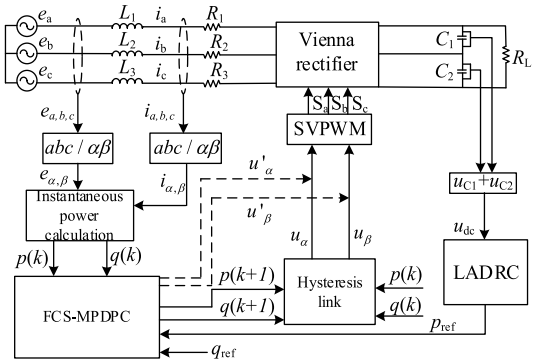

FIGURE 7. Novel optimal voltage vector selection control block diagram.

Under the same time k, the smaller the absolute value of the slope of the power change starting from time k, the later it reaches the upper and lower limits of the power, and the longer the step length is. Hence, the extension length of active power in hysteresis loop can be obtained as follows:

$$p_{exten} = \begin{cases} p_{exten}^{right}, & p_{exten}^{right} > p_{exten}^{left} \\ p_{exten}^{left}, & p_{exten}^{right} < p_{exten}^{left} \end{cases} \tag{11}$$

The hysteresis loop and step calculation of reactive power construction are consistent with those of active power.

Finally, the optimal output voltage vector will be determined based on the one that maximizes the sum of active and reactive power extensions across all the steps. After introducing the hysteresis loop, the selection of the optimal voltage vector is no longer based solely on the minimum tracking error.

In addition to the above ideal operating state, the active and reactive power obtained at time $k+1$ are likely to be outside the hysteresis loop. To address this situation, the part outside the hysteresis loop employs the traditional FCS-MPDPC to obtain the optimal voltage vectors u'_α and u'_β. The part within the hysteresis loop performs the novel optimal voltage vector selection control to acquire the optimal voltage vectors u_α and u_β. Fig. 7 presents the overall control block diagram of the system, and Fig. 8 is the flow chart of the proposed algorithm.

V. SIMULATION AND EXPERIMENTAL VERIFICATIO

In order to verify the feasibility of the proposed control strategy, a novel control strategy simulation model was established in the Matlab/Simulink environment. Furthermore, an experiment platform for Vienna rectifier based on dSPACE was built for experimental verification. The simulation model was consistent with the device parameters used in the experimental platform, as specific parameter values are shown in Tab. 1.

A. SIMULATION ANALYSIS

Firstly, the steady state performance of the system under the control strategy is verified. Fig. 9 shows the simulation analysis of the input current and output voltage of the system when the novel vector selection control strategy is adopted.

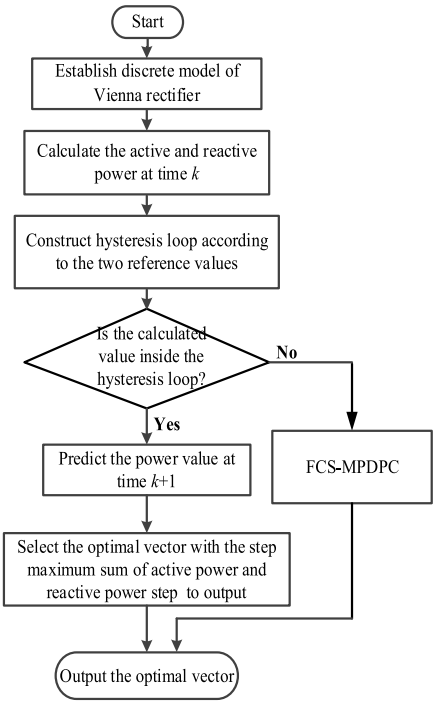

FIGURE 8. Novel optimal voltage vector selection control flow chart.

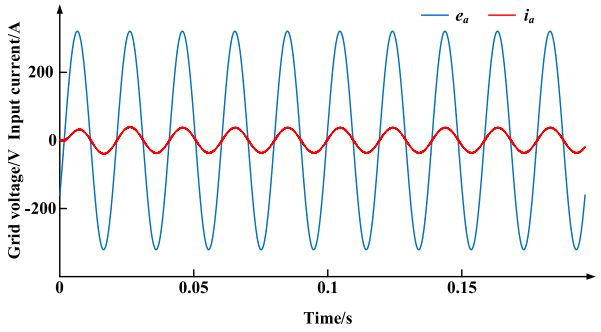

a. A-phase voltage, A-phase current

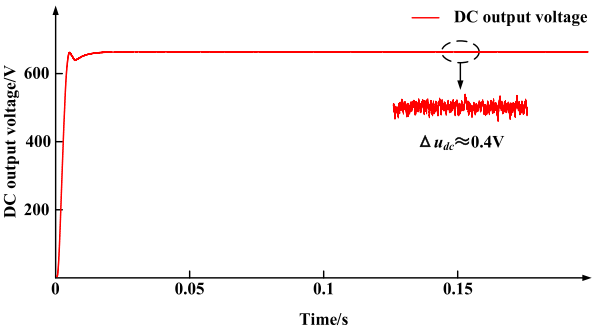

b. Output voltage

FIGURE 9. Steady state simulation analysis of the system.

It can be seen from Fig. 9 (a) that the input current under the control of the novel optimal voltage vector selection can follow the grid voltage well, achieving the purpose of unit power factor operation. At the same time, because the outer loop of this control strategy adopts linear active disturbance rejection control (LADRC), the output voltage in Fig. 9 (b)

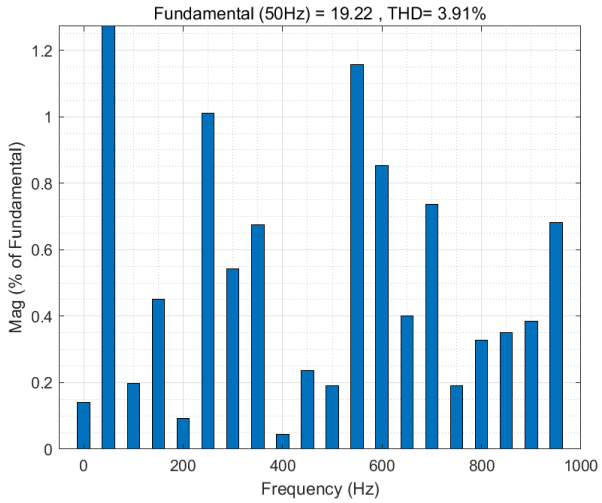

a. A-phase current THD with FCS-MPDPC
（A-phase current THD with hysteresis width of 0）

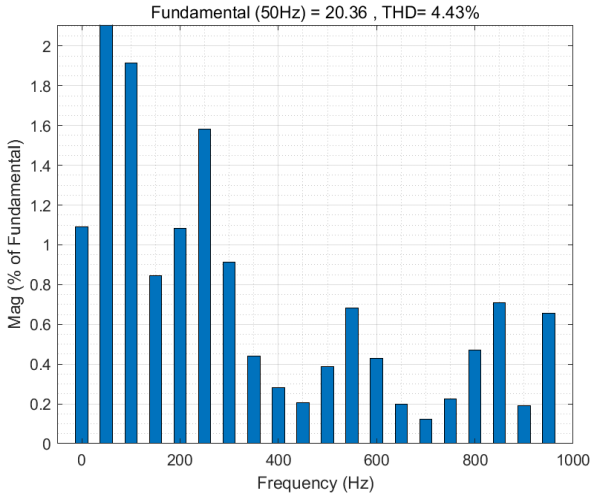

b. A-phase current THD with hysteresis width increase 10%

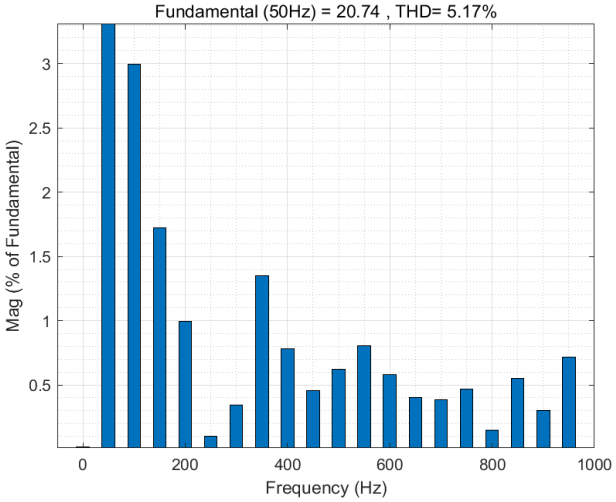

c. A-phase current THD with hysteresis width increase 20%

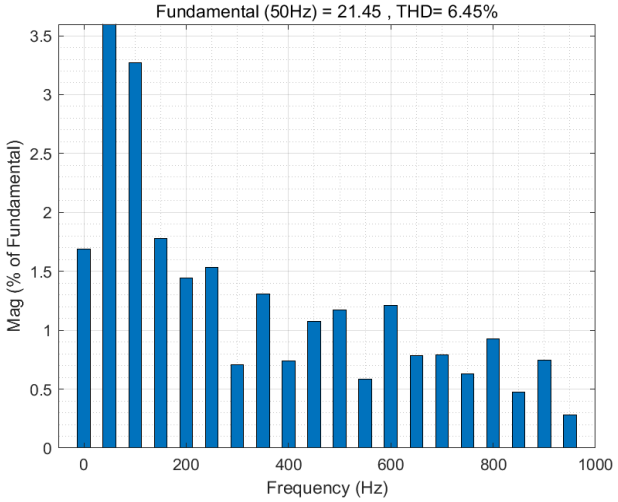

d. A-phase current THD with hysteresis width increase 30%

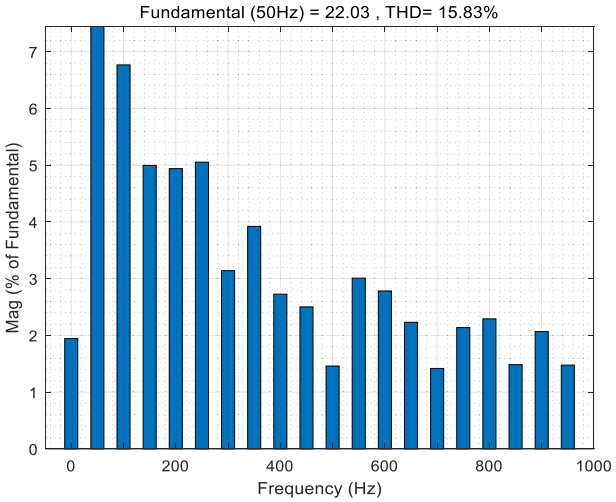

e. A-phase current THD with hysteresis width increase 50%

FIGURE 10. **Simulation analysis of THD under different hysteresis widths.**

TABLE 1. Vienna rectifier parameter value.

Parameters	Values
Effective value of input phase voltage e	220V
The output voltage u_{dc}	650V
Filtering inductance L	5mH
DC-bus capacitor C_1、C_2	3300μF
Power reference value P_{ref}	7kW
Initial hysteresis width h	0.35kW
Switching frequency with FCS-MPDPC f	20kHz

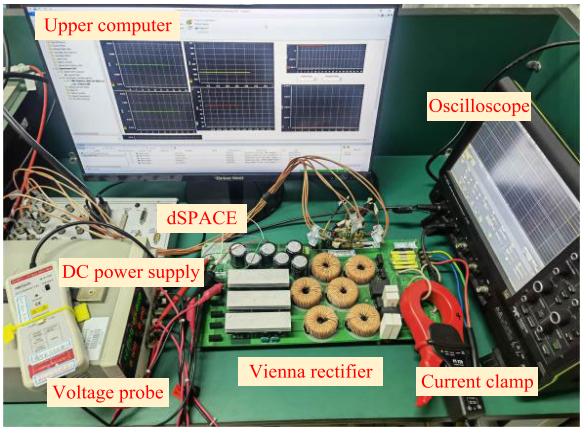

FIGURE 11. Vienna rectifier experiment platform.

TABLE 2. Comparison of performance under different hysteresis widths.

Hysteresis width	Switching frequency	THD
0	20000Hz	3.91%
Increase 10%	18506Hz	4.43%
Increase 20%	15098Hz	5.17%
Increase 30%	11556Hz	6.45%
Increase 50%	10893Hz	15.83%

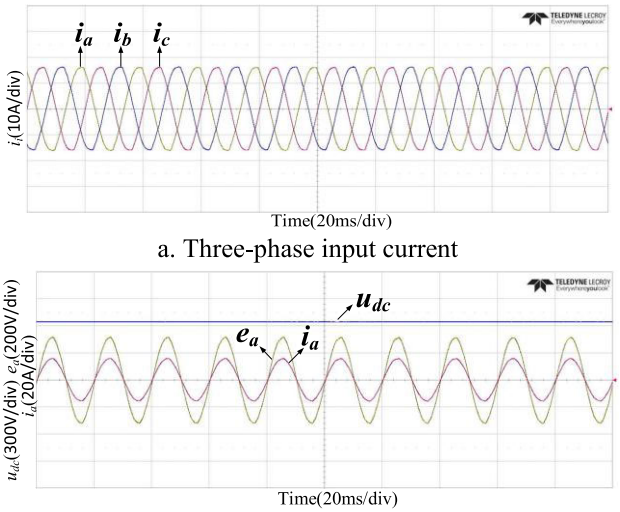

a. Three-phase input current

b. A-phase voltage, A-phase current, output voltage

FIGURE 12. Steady state experimental analysis of the system.

can quickly reach the given voltage value of 650V without overshooting, and the voltage fluctuation after stabilization is maintained at about 0.4V, which is in accordance with the relevant regulations of output DC voltage.

In the hysteresis control described above, the hysteresis width affects the switching frequency and the THD of the input current. The relationship between them is as follows: as the hysteresis width increases, the switching frequency decreases and the distortion rate increases, so there are some contradictions between them. In order to verify the significant changes of the proposed control strategy and the traditional FCS-MPDPC in the THD and switching frequency of the input current, and to verify the influence of different hysteresis widths on the THD and switching frequency of the Vienna rectifier, the hysteresis width was increased by 10%, 20%, 30% and 50%, after setting the bandwidth h.

Both the input current THD and switching frequency are important indicators for measuring the efficient operation of the Vienna rectifier [23]. As shown in Tab.2, the variation trends of the Vienna rectifier switching frequency and THD are under five different hysteresis widths when the novel optimal voltage vector selection control strategy is adopted.

According to the data in Tab. 2, compared with the traditional FCS-MPDPC, that is, when the hysteresis width is 0, the control strategy proposed in this paper can effectively reduce the switching frequency of the system. In addition, when the hysteresis width is in the range of 0 to 30%, the proposed control strategy can reduce the switching frequency while slightly increasing the THD of the input current. However, when the hysteresis width increases beyond 30%, the THD cannot meet the relevant requirements, which is not conducive to the operation of the system. Therefore, it can be concluded that when the hysteresis width is increased by 20%, that is, when the power fluctuation is between 6580W-7420W, the steady state performance of the system is the best, and the input current THD is acceptable while the switching frequency is reduced. Finally, the introduction of hysteresis link in the model predictive control can effectively solve the contradiction between the input current THD and switching frequency, which is another advantage of the control strategy proposed in this paper.

B. EXPERIMENTAL ANALYSIS

This section verifies the feasibility of the proposed control strategy through experiments. Fig.11 illustrates the Vienna rectifier experimental platform. Firstly, the steady state performance of the system under the control strategy is verified. Then, the significant variations of the proposed control strategy and FCS-MPDPC in the THD of input current and switching frequency are analyzed, as well as the effects of different hysteresis widths on the THD and switching frequency of the Vienna rectifier.

The experimental waveform of the system operating in steady state is shown in Fig. 12, where i_i represent the three-phase input current, u_{dc} represents the DC side output voltage, and e_a represents the A-phase grid voltage.

As can be seen from Fig. 12, the output voltage of Vienna rectifier running in steady state is stable at the given value

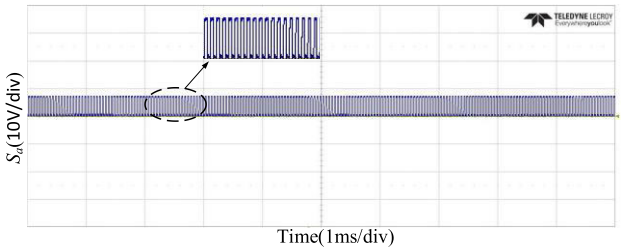

a. Switching frequency with traditional FCS-MPDPC (Switching frequency with hysteresis width of 0)

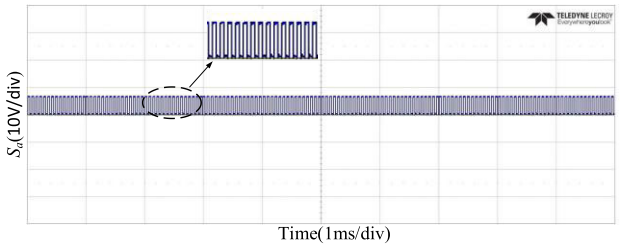

b. Switching frequency with hysteresis width increase 20%

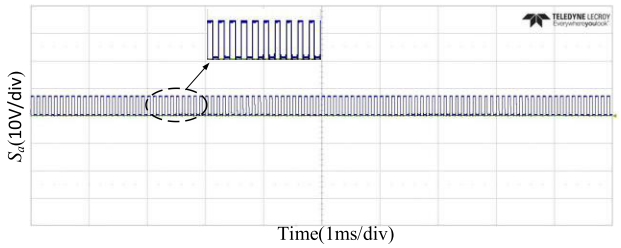

c. Switching frequency with hysteresis width increase 50%

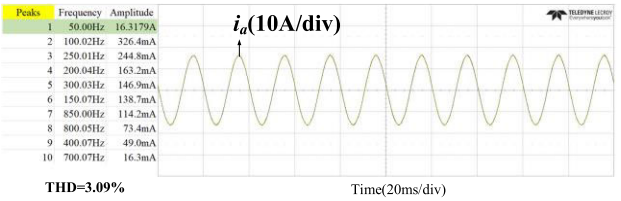

d. A-phase current with traditional FCS-MPDPC (A-phase current with hysteresis width of 0)

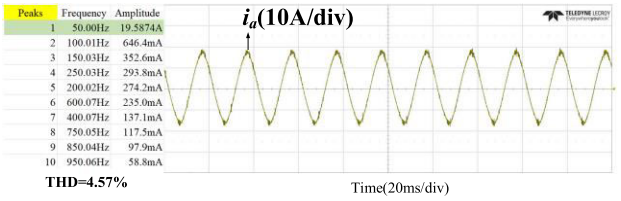

e. A-phase current with hysteresis width increase 20%

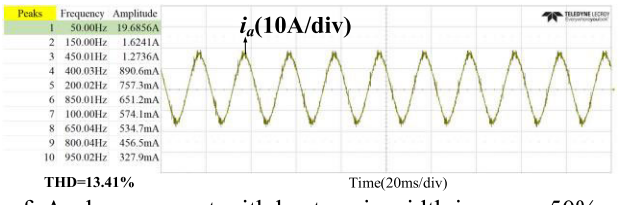

f. A-phase current with hysteresis width increase 50%

FIGURE 13. Experimental waveforms at different hysteresis widths.

of 650V, the input current is maintained at approximately 18A, and the A-phase grid voltage and A-phase input current operate in the same phase, thus achieving the purpose of unit power factor operation. The experimental results confirm the effectiveness of the control strategy.

In order to verify the superiority of the proposed control strategy, the influence of different hysteresis widths on the overall performance of the system in actual operation is also evaluated. Therefore, experiments are conducted to compare the A-phase switching frequency and THD of the input current for FCS-MPDPC and hysteresis control with different widths.

As can be seen from Fig. 13, when the hysteresis width is 0, that is, when the FCS-MPDPC is used to control, the switching frequency of phase A is approximately 20,000 Hz. When the hysteresis width is increased by 20%, that is, when the novel optimal voltage vector selection is used to control, the switching frequency of phase A is around 15000Hz. When the hysteresis width is increased by 50%, the switching frequency of phase A is about 10000Hz, and the switching frequency of the system has been effectively reduced after the novel vector preferred control. Moreover, the THD of the input current in operation at different widths of hysteresis increases with the increase of the width, which is in agreement with the above analysis results. The results are 3.09%, 4.57% and 13.41%, respectively. Notably, when the width increases from 20% to 50%, the THD of the current increases sharply. Therefore, it can be seen that not necessarily the larger the hysteresis width is, the better the control effect is. Consequently, the final choice is an increase of the bandwidth of 20%, through which the current distortion rate and switching frequency of the system best meet the required requirements.

VI. CONCLUSION

The novel optimal voltage vector selection control strategy changes the objective function selection criterion, which is commonly used in Vienna rectifier. By introducing hysteresis loop into the traditional FCS-MPDPC, this optimal method is redefined to select the most suitable voltage vector, thus keeping the switching frequency of the system at a low operating state while slightly increasing the THD of the input current. From this point of view, the proposed control can be used to effectively resolve the contradiction between the input current THD and switching frequency in traditional FCS-MPDPC, with a wide application value.

REFERENCES

[1] A. Khaligh and S. Dusmez, "Comprehensive topological analysis of conductive and inductive charging solutions for plug-in electric vehicles," *IEEE Trans. Veh. Technol.*, vol. 61, no. 8, pp. 3475–3489, Oct. 2012, doi: 10.1109/TVT.2012.2213104.

[2] H. Chen and D. C. Aliprantis, "Analysis of squirrel-cage induction generator with Vienna rectifier for wind energy conversion system," *IEEE Trans. Energy Convers.*, vol. 26, no. 3, pp. 967–975, Sep. 2011, doi: 10.1109/TEC.2011.2143414.

[3] X. Chen, Y. Wang, W. Song, and G. Ma, "High-frequency switching rectifier module for high-voltage DC communication power supply," *Trans. China Electrotech. Soc.*, vol. 29, no. 4, pp. 152–159, Apr. 2014, doi: 10.19595/j.cnki.1000-6753.tces.2014.04.020.

[4] J. Rodriguez, M. P. Kazmierkowski, J. R. Espinoza, P. Zanchetta, H. Abu-Rub, H. A. Young, and C. A. Rojas, "State of the art of finite control set model predictive control in power electronics," *IEEE Trans. Ind. Informat.*, vol. 9, no. 2, pp. 1003–1016, May 2013, doi: 10.1109/TII.2012.2221469.

[5] P. Cortes, S. Kouro, B. La Rocca, R. Vargas, J. Rodriguez, J. I. Leon, S. Vazquez, and L. G. Franquelo, "Guidelines for weighting factors design in model predictive control of power converters and drives," in *Proc. IEEE Int. Conf. Ind. Technol.*, Gippsland, VIC, Australia, Feb. 2009, pp. 1–7.

[6] S. A. Davari, D. A. Khaburi, and R. Kennel, "An improved FCS–MPC algorithm for an induction motor with an imposed optimized weighting factor," *IEEE Trans. Power Electron.*, vol. 27, no. 3, pp. 1540–1551, Mar. 2012, doi: 10.1109/TPEL.2011.2162343.

[7] C. A. Rojas, J. Rodriguez, F. Villarroel, J. R. Espinoza, C. A. Silva, and M. Trincado, "Predictive torque and flux control without weighting factors," *IEEE Trans. Ind. Electron.*, vol. 60, no. 2, pp. 681–690, Feb. 2013, doi: 10.1109/TIE.2012.2206344.

[8] R. Gregor, F. Barrero, S. L. Toral, M. J. Duran, M. R. Arahal, J. Prieto, and J. L. Mora, "Predictive-space vector PWM current control method for asymmetrical dual three-phase induction motor drives," *IET Electr. Power Appl.*, vol. 4, no. 1, pp. 26–34, Jan. 2010, doi: 10.1049/iet-epa.2008.0274.

[9] S. Vazquez, J. I. Leon, L. G. Franquelo, J. M. Carrasco, O. Martinez, J. Rodriguez, P. Cortes, and S. Kouro, "Model predictive control with constant switching frequency using a discrete space vector modulation with virtual state vectors," in *Proc. IEEE Int. Conf. Ind. Technol.*, Gippsland, VIC, Australia, Feb. 2009, pp. 1–6.

[10] M. A. Pérez, P. Cortés, and J. Rodríguez, "Predictive control algorithm technique for multilevel asymmetric cascaded H-bridge inverters," *IEEE Trans. Ind. Electron.*, vol. 55, no. 12, pp. 4354–4361, Dec. 2008, doi: 10.1109/TIE.2008.2006948.

[11] C. Xia, T. Liu, T. Shi, and Z. Song, "A simplified finite-control-set model-predictive control for power converters," *IEEE Trans. Ind. Informat.*, vol. 10, no. 2, pp. 991–1002, May 2014, doi: 10.1109/TII.2013.2284558.

[12] X. Feng, Y. Sun, X. Cui, W. Ma, and Y. Wang, "A compound control strategy of three-phase Vienna rectifier under unbalanced grid voltage," *IET Power Electron.*, vol. 14, no. 16, pp. 2574–2584, Dec. 2021, doi: 10.1049/pel2.12202.

[13] W. Song and Z. Deng, "Model predictive power control scheme for single-phase PWM rectifiers with constant switching frequency," *Electr. Mach. Control*, vol. 20, no. 4, pp. 93–100, Apr. 2016, doi: 10.15938/j.emc.2016.04.013.

[14] J. Lee, K. Lee, and F. Blaabjerg, "Predictive control with discrete space-vector modulation of Vienna rectifier for driving PMSG of wind turbine systems," *IEEE Trans. Power Electron.*, vol. 34, no. 12, pp. 12368–12383, Dec. 2019, doi: 10.1109/TPEL.2019.2905843.

[15] X. Yang, S. Yang, T. Wang, Y. Xu, H. Li, and A. Yu, "Constant-frequency model predictive control based on power tracking objective function for three-phase PWM rectifier," *Power Syst. Technol.*, vol. 45, no. 3, pp. 1125–1131, Mar. 2021, doi: 10.13335/j.1000-3673.pst.2019.1095.

[16] X. Feng, X. Cui, W. Ma, S. Wang, and K. Zhang, "Double closed-loop control strategy of three-phase Vienna rectifier based on unbalanced power grid," *Power Syst. Technol.*, vol. 45, no. 5, pp. 1976–1984, May 2021, doi: 10.13335/j.1000-3673.pst.2020.1221.

[17] W. Zhu, C. Chen, and S. Duan, "A model predictive control method with discrete space vector modulation of Vienna rectifier," *Proc. CSEE*, vol. 39, no. 20, pp. 6008–6016 and 6181, Oct. 2019, doi: 10.13334/j.0258-8013.pcsee.182059.

[18] W. Song, J. Huang, Y. Zhong, and L. Wang, "A hysteresis current control method with neutral point potential balancing control for Vienna rectifier," *Power Syst. Technol.*, vol. 37, no. 7, pp. 1909–1914, Jul. 2013, doi: 10.13335/j.1000-3673.pst.2013.07.033.

[19] H. Zhao, Y. Li, J. Du, Q. Zheng, D. Li, and P. Shi, "A voltage vector-based sine-like hysteresis current control strategy," *Power Syst. Technol.*, vol. 42, no. 2, pp. 628–636, Feb. 2018, doi: 10.13335/j.1000-3673.pst.2017.0210.

[20] A. I. Maswood, E. Ai-Ammar, and F. Liu, "Average and hysteresis current-controlled three-phase three-level unity power factor rectifier operation and performance," *IET Power Electron.*, vol. 4, no. 7, pp. 752–758, Aug. 2011, doi: 10.1049/iet-pel.2010.0189.

[21] T. Dragicevic and M. Novak, "Weighting factor design in model predictive control of power electronic converters: An artificial neural network approach," *IEEE Trans. Ind. Electron.*, vol. 66, no. 11, pp. 8870–8880, Nov. 2019, doi: 10.1109/TIE.2018.2875660.

[22] T. Geyer, *Model Predictive Control of High Power Converters and Industrial Drives*. Chichester, U.K.: Wiley, 2016.

[23] L. Feng, J. Fu, L. Liao, Y. Wen, and W. Song, "An improved low switching frequency model predictive direct torque control strategy for traction permanent magnet synchronous motor," *Proc. CSEE*, vol. 41, no. 21, pp. 7507–7516, Nov. 2021, doi: 10.13334/j.0258-8013.pcsee.211266.

YONGMING SUN was born in China, in 1997. He received the B.S. degree in electrical engineering and automation from the College of Electronic Information Engineering, Taiyuan University of Science and Technology, Taiyuan, China, in 2020. He is currently pursuing the M.S. degree in electrical engineering with the China University of Petroleum (East China).

His research interest includes the control strategy of Vienna rectifier.

XINGTIAN FENG received the B.S. and M.S. degrees in electrical engineering from the China University of Petroleum (East China), Qingdao, China, in 2001 and 2004, respectively, and the Ph.D. degree in electrical engineering from the Institute of Electrical Engineering, Chinese Academy of Sciences (CAS), Beijing, China, in 2012.

Since 2004, he has been with the China University of Petroleum (East China). His research interests include power electronics, power quality, distributed generation, and energy storage technology.

ZHANJIANG DAI was born in China, in 1999. He received the B.S. degree from the College of New Energy, China University of Petroleum (East China), Qingdao, China, in 2021, where he is currently pursuing the M.S. degree.

His current research interests include power electronics converters and model predictive control.

WENZHONG MA received the B.S. and M.S. degrees in electrical engineering from the Harbin Institute of Technology (HIT), Harbin, China, in 1993 and 1995, respectively, and the Ph.D. degree in electrical engineering from the Institute of Electrical Engineering, Chinese Academy of Sciences (CAS), Beijing, China, in 2006.

He was a Visiting Professor with the University of Alberta, Edmonton, AB, Canada, from 2013 to 2014. Since 1995, he has been a Faculty Member with the China University of Petroleum, Qingdao, China, where he is currently a Professor with the Department of Electrical Engineering. He has done extensive research in electrical engineering and automation, including power electronic systems, converters, renewable energy, distributed micro grid, HVdc, motor design, and motor drives. From 2002 to 2006, he was involved in a National Key Project for Shanghai High-Speed Maglev Train Systems, which is the first commercial high-speed maglev train. He took charge of the commissioning and testing work of the long stator linear motor, propulsion system, and power distribution systems. He is the holder of six patents in his areas of interest. He has authored six books and authored or coauthored more than 30 technical papers.

Dr. Ma is a Committee Member of the China Electrotechnical Society (CES).